

# Grover-like search via Frenkel exciton trapping mechanism

A. Thilagam\*

*Applied Centre for Structural and Synchrotron Studies,  
University of South Australia, Mawson Lakes, SA 5095, Australia*

(Dated: October 16, 2018)

We propose the physical implementation of a Grover-like search problem by means of Frenkel exciton trapping at a shallow isotopic impurity against a background of competing mechanisms. The search culminating at the impurity molecule, designated the “winner” site, is marked by its enhanced interaction with acoustic phonons at low temperatures. The quantum search proceeds with the assistance of an Oracle-like exciton-phonon interaction which addresses only the impurity site, via the Dyson propagator within the Green’s function formalism. The optimum parameters of a graph lattice with long-range intersite interactions required to trap the exciton in the fastest time are determined, and estimates of error rates for the naphthalene doped organic system are evaluated. We extend analysis of quantum search to a fluctuating long-range interacting cycle (LRIC) graph lattice system.

PACS numbers: 03.65.Yz, 03.65.Ud, 03.67.Mn

## INTRODUCTION

Quantum search via Grover’s algorithm [1] provides one possible framework by which combinatorial search can be speeded up considerably over those employing classical rules. For a function  $f(x) : \{1, \dots, N\} \rightarrow \{0, 1\}$  where  $f(x) = 0$  for  $x \neq w$  and  $f(x) = 1$  for  $x = w$ , the algorithm locates the “winner”  $w$  using of order  $\sqrt{N}$  queries for spatial dimensions exceeding two [2]. The successful bid is generally represented by an oracle  $U_w$  with  $U_w|x\rangle = (-1)^{f(x)}|x\rangle$ , and is sometimes treated as a black box which returns the value 1 for a particular one or a small set of inputs. The possibility of widening the choices for quantum searches via use of quantum random walks was first proposed by Farhi and Gutmann [3] who showed that the time taken to move from one point of a graph vertex to another is exponentially faster for a walker following quantum rules over one who obeys classical physics. Unlike their classical counterparts, paths in quantum walks can interfere leading to nonexistence of a quantum walker at a vertex.

In the continuous-time quantum walk formulation [4], a Hamiltonian with oracle-like properties,  $H_w = 1 - |w\rangle\langle w|$  is employed with  $|w\rangle$  as the unknown state. Under this formalism, the ground state of the Hamiltonian is taken as  $|w\rangle$  while all other equivalent but orthogonal states are considered as undesired outcomes of the search. Instead of the counting procedure, the efficiency of the search is quantified by the time taken to locate ground state  $|w\rangle$ .

In this work we attempt implementation of Grover’s search via the Frenkel exciton, a bound system of electron and hole which propagates from one site to another in a quasi one-dimensional system of  $N$  molecular sites. Frenkel excitons are also modeled as delocalized excitation over the real crystal space [5], and as noninteracting fermions [6], the exciton is thus an ideal example of an extended entangled system. We consider the exciton transfer mechanism as analogous to a quantum walker on a graph  $G$  where each vertex point represents a lattice site. The route of propagation of the exciton from one site to another is given by the edge joining one vertex to another with the number of edges incident on a specific vertex considerably being simplified for one dimensional systems. During a quantum search on graphs, a particular vertex is distinguished from all others and a successful outcome occurs when this vertex is reached. We examine the physical implementation of Grover’s search by designating an impurity molecule as the “winner” located at the special vertex. The impurity site thus mimics the role of the desired outcome  $|w\rangle$ . The impurity molecule is distinguished from other molecules via the assistance of lattice vibrations, so that the difference between the energy band with and without the impurity present is accounted for by phonons. We note the fine balance involved in locating the impurity molecule, while lattice vibrations are needed to define vital properties of the impurity molecule, they should not be strong enough to hamper the search. The analysis can be extended to the existence of more than one impurity atoms, however we restrict our case to a single “winner”.

## EXCITON TRAPPING MECHANISM

The trapping of excitons in molecular crystals has been well documented in the literature [5]. The overlap of intermolecular wavefunctions is weak in organic molecular crystal systems such as anthracene and naphthalene [5], electronic wavefunctions are thus localized at individual molecular sites. The exact form of these functions are not

needed to derive salient properties of Frenkel excitons, however every molecular site has an equal probability of being excited by an incident photon due translation symmetry, a salient feature which has important implications for quantum parallelism. While a Frenkel exciton can be visualized as being smeared out in space, it can also be modeled as a bound electron-hole quasiparticle hopping from one site to another.

Trapping sites are categorized as either impurity molecules (chemical traps) or dislocated molecules (physical traps), with the trap state assumed to be lower than the initial exciton state by an energy known as the trap depth. The excess energy is absorbed by phonons associated with lattice vibrations, the trapping mechanism thus occurring as a result of coupling between the exciton and phonons. A transition from a delocalized exciton state to a localized exciton state occurs at specific molecular sites. The extend by which neighboring lattice structure is altered depends on the magnitude of trap depth. A shallow isotopic impurity participates in the dynamics of the delocalized states of the host lattice system, unlike a deep impurity state. The energy state of the deep impurity falls far beyond the energy band states of the host molecular system. In this work, we consider introduction of a shallow isotopic impurity which alters the crystal symmetry only marginally, but one that eventually traps an exciton in the final state. We thus assume that the trap depth is present in the range of phonon bandwidths, so that a single phonon separates the host band and impurity trap. The trap depth may be viewed as a point of maximal lattice relaxation, with the excitation moving from an unrelaxed lattice structure to the relaxed lattice state at the impurity site, the surplus energy being converted into lattice energy. The discrete exciton spectrum in a finite one dimensional crystal system differs from the continuous spectrum of the infinite 1D system. Hence a single discrete level corresponding to the self-trapped state remains distinct in the infinite chain unlike the discrete energy levels of the finite chain.

We note that an initially delocalized exciton examines all of the sites simultaneously in a superposed form before reaching its target. The exciton lifetime therefore yields a measure of the efficiency of search from a quantum-information perspective. The absorption of a photon prior to search triggers the initialization process whereby an equal weighted superposition of all states is created. The exciton eigenvector appear as

$$|\mathbf{K}\rangle = N^{-1/2} \sum_{\mathbf{l}} e^{i\mathbf{K}\cdot\mathbf{l}} B_{\mathbf{l}}^{\dagger} |\mathbf{0}\rangle \quad (1)$$

where  $\mathbf{K}$  is reciprocal lattice vector,  $|\mathbf{0}\rangle$  is the vacuum state with all molecules in ground state and  $B_{\mathbf{l}}^{\dagger}$  is the creation operator of exciton at position coordinate  $\mathbf{l}$ .  $N$  is the number of unit cells in the crystal which increases with the number of molecules for each unit cell. We note that Eq. (1) is the result of a single step of a naturally occurring process involving photon absorption that require the equivalent of  $\log_2(N) + 1$  qubits to store the superposed state. In Eq. (1), we have dropped notations associated with the exciton spin, however we will consider spin indices in mechanisms involving exciton formation and annihilation in forthcoming sections of this work.

The Frenkel exciton creation operator with wavevector  $\mathbf{K}$  can be easily obtained using the Fourier transform of Eq. (1)

$$B_{\mathbf{K}}^{\dagger} = N^{-1/2} \sum_{\mathbf{l}} e^{i\mathbf{K}\cdot\mathbf{l}} B_{\mathbf{l}}^{\dagger} \quad (2)$$

The exciton creation operator  $B_{\mathbf{K}}^{\dagger}$  localized in  $\mathbf{K}$ -space is delocalized in real space [5]. The motion of the exciton in molecular systems is governed by an Hamiltonian derived using a tight-binding model [5, 7, 8]

$$\hat{H}_{ex} = \sum_{\mathbf{l}} \left( \Delta E + \sum_{\mathbf{m} \neq \mathbf{l}} D_{\mathbf{l},\mathbf{m}} \right) B_{\mathbf{l}}^{\dagger} B_{\mathbf{l}} + \sum_{\mathbf{m} \neq \mathbf{l}} M_{\mathbf{l},\mathbf{m}} B_{\mathbf{l}}^{\dagger} B_{\mathbf{m}} \quad (3)$$

where  $\Delta E$ , the on-site (intra-site) excitation energy at equilibrium is the same at all sites due to translational symmetry.  $D_{\mathbf{l},\mathbf{m}}$  is the dispersive interaction matrix element which determines the energy difference between a pair of excited electron and hole at a molecular site and ground state electrons at neighboring sites [5, 7].  $M_{\mathbf{l},\mathbf{m}}$  the electron transfer matrix element between molecular sites at  $\mathbf{l}$  and  $\mathbf{m}$ . Using Eq. (2), we obtain a Hamiltonian diagonal in  $\mathbf{K}$  space

$$\hat{H}_{ex} = \sum_{\mathbf{k}} E_0(\mathbf{k}) B_{\mathbf{k}}^{\dagger} B_{\mathbf{k}} \quad (4)$$

$$E_0(\mathbf{k}) = \Delta E + \sum_{\mathbf{m} \neq \mathbf{0}} D_{\mathbf{0},\mathbf{m}} + M_{\mathbf{0},\mathbf{m}} \exp(i\mathbf{k}\cdot\mathbf{m}) \quad (5)$$

where  $E_0(\mathbf{k})$  is energy of the exciton of wavevector  $\mathbf{k}$  and subscript 0 denotes the absence of lattice site fluctuations. For simple  $d$ -dimensional lattice with nearest neighbor transfer energy  $M_{1,\mathbf{m}} \sim J$ , we obtain the well known dispersion relation  $E_0(\mathbf{K}) = \Delta E + 2J \sum_{i=1}^d \cos(K_i)$  with the exciton band extending from  $\Delta E - B$  to  $\Delta E + B$ .  $B = 2Jd$  denotes the half band width and we emphasize its critical dependence on efficiency of exciton transport on designated graph structure of molecular sites.

### Excitonic bandwidth in graph lattice with long-range intersite interactions

The bandwidth  $B$  which is determined by the energy span of the host lattice over a spectrum of wavevectors, is a vital property of the exciton. It influences excitonic coherence quantities such as its delocalization length and relaxation mechanism, and provides a measure of time needed for the exciton to move away from its initial site of excitation. It is intimately linked with arrangement of superpositions of single-site excitations of the initial state. In a recent work on photosynthetic organic systems [9], it was shown that the efficiency of excitation transfer depends both on the symmetry properties of such superposition states and on the number of sites among which the excitation is initially delocalized, with results showing an optimal delocalization length for which transfer time is a minimum. To illustrate the dependence of the trapping time on size-effects associated with long-range excitonic coherences as well as underlying structure of the lattice points, we consider transfer matrix element  $M_{1,\mathbf{m}}$  of the form

$$M_{1,\mathbf{m}} = \frac{J}{|m-l|^\mu} \quad (6)$$

where  $M_{\mathbf{m},\mathbf{m}} = 0$  and intersite energy term  $J > 0$ . This form of the matrix element has recently been shown to reveal various rich and interesting properties for a select range of  $1 < \mu < \frac{3}{2}$  [11–13]. In the absence of lattice vibrations, the eigenstates of Eq. (3) form waves with momenta  $K = \frac{2\pi k}{N}$  within the Brillouin zone  $k \in [-\frac{N}{2}, \frac{N}{2}]$  with energies

$$\begin{aligned} E(K) &= 2J \sum_{n=1}^N \frac{\cos(Kn)}{|n|^\mu} \\ &= \sum_{s=+,-} \text{Li}_\mu(e^{iKs}) - \sum_{s=+,-} e^{i(N+1)Ks} \Psi(e^{iKs}, \mu, N+1) \end{aligned} \quad (7)$$

where  $\text{Li}_\mu(a)$  is the Polylogarithm function and  $\Psi(z, \mu, a)$  is the Lerch transcendent function [10]. In the limit where  $K \rightarrow 0$  which occurs at the upper band edge, we use a simplified dispersion relation obtained as  $E_K = E_0(\mu) - JA(\mu)|K|^{\mu-1}$  [11] where  $E_0(\mu)$  is the upper band-edge energy and  $A(\mu)$  is a dimensionless constant.  $E_0(\mu)$  and  $A(\mu)$  can be obtained using series expansion of Eq. (7). An approximate but simple relation between the bandwidth and system size  $N$  follows at the upper band edge ( $1 < \mu < \frac{3}{2}$ )

$$B(K \rightarrow 0, N \rightarrow \infty) \approx E_0(\mu)(1 - A(\mu)'N^{1-\mu}) \quad (8)$$

where  $A(\mu)' < 1$  is a small dimensionless quantity. While the states are extended over the whole crystal structure at  $\mu < \frac{3}{2}$ , it has been shown that localization effects appear for higher values of  $\mu$  for systems with *uncorrelated* diagonal disorder and long-range coupling of the form in Eq. (6) [11]. We note that lattice vibrations, as considered in our work, provide a fabric of *correlated* diagonal disorder and therefore localization effects may be present with properties different from those obtained by Rodríguez et al [11]. Nonetheless, we consider that the system obeying long-range coupling of the form in Eq. (6) still undergoes vital changes at the critical point when  $\mu = \frac{3}{2}$

### ESTIMATING SEARCH TIME USING GREEN'S FUNCTIONS.

Implementation of the quantum search process involves the following crystal Hamiltonian with the impurity at site  $w$

$$\hat{H}_T = \hat{H}_0 + \hat{H}_w \quad (9)$$

$$\hat{H}_0 = \hat{H}_{ex} + \sum_{\mathbf{q}} \hbar\omega(\mathbf{q}) b_{\mathbf{q}}^\dagger b_{\mathbf{q}}$$

$$\hat{H}_w = \Delta p B_w^\dagger B_w \quad (10)$$

where  $\hat{H}_{ex}$  is given in Eq. (4) and the second term in  $\hat{H}_0$  denotes the phonon energies.  $\hat{H}_0$  correspond to a impurity-free lattice structure.  $\hat{H}_w$  denotes a trapped exciton at site  $w$ , with trap depth  $\Delta p$  defined as the difference between a state of zero phonon and one where interactions between exciton and phonons leading to absorption of a phonon is optimum. We consider the presence of just one impurity site and assume that the translational symmetry of the molecular system is left intact. This is justified for isotopic impurities which mimic the molecular structure of the host molecules quite well. We note that the lowered energy  $\Delta p$  associated with the Hamiltonian  $\hat{H}_w$  effectively marks the searched state,  $|w\rangle$ . As discussed in Ref. [14], solving the Grover's problem involves the determination of the lowered energy, and hence energy of the Hamiltonian in Eq. (9). This translates to evaluation of the trapping time of an exciton initially located at a site other than at  $|w\rangle$ .

We emphasize that the driving term  $\sum_{\mathbf{q}} \hbar\omega(\mathbf{q})b_{\mathbf{q}}^\dagger b_{\mathbf{q}}$  associated with a background of boson bath assist with the Oracle search operation. A resonant coupling term associated with exciton-phonon interaction at all host sites has been intentionally left out in Eq. (9). This is based on the assumed presence of an Oracle-like mechanism which ensures that all phonon-assisted relaxation (one-phonon emission and Raman processes) cumulates at the impurity site, bypassing other lower energy sites, during the search process. An Oracle is a component of an algorithm which can be regarded as a "black box" that recognizes solutions to a given problem [15]. The inner dynamics of the Oracle is generally unknown, however at very low temperatures its inner workings appears almost apparent. Raising the temperature of the crystal medium therefore involves the risk of the Oracle malfunctioning, as will be shown in detailed evaluations in the next Section. We therefore address the impurity trapping problem at very low temperatures (close to 0K), a limit in which the mean-free path associated with phonon scattering is large due to a linear scaling of exciton scattering rate with temperature. The exciton is more likely to be trapped at the impurity site than to bypass it. Various other competing mechanisms which act to disrupt the search and introduce errors will also be discussed subsequent to the current Section.

The exciton-phonon coupling Hamiltonian associated with the interaction between the exciton at site  $w$  and phonons can be written as [5]

$$\hat{H}_{exp} = B_w^\dagger B_w \sum_{\mathbf{q}} \chi(q)(b_{\mathbf{q}}^\dagger + b_{\mathbf{q}}) \quad (11)$$

where coupling function  $\chi(q)$  arises due to acoustic phonons dominant at low temperatures.  $\chi(q)$  is dependent only on the phonon wavevector  $q$

$$\begin{aligned} \chi(q)^2 &= \frac{1}{N} \hbar\omega(\mathbf{q}) E_{LR} \\ E_{LR} &= \frac{E_D^2}{2Iv^2} \end{aligned} \quad (12)$$

where phonon frequency  $\omega(\mathbf{q}) = v|q|$ ,  $v$  being the velocity of sound in the crystal medium and  $E_{LR}$  is the lattice relaxation energy.  $I$  is the mass coefficient of host molecules, taken as almost the same as that of the impurity and deformation potential  $E_D$  remains an invariant throughout all lattice sites. A coupling coefficient  $\gamma = E_{LR}/B$  yields a measure of the scattering regime of the crystal system. For strong lattice vibrations at high  $\gamma$ , the exciton is less likely to hop and tends to remain localized at its initial site. At small  $\gamma$ , the exciton is in a delocalized state, until it reaches the site at  $|w\rangle$ . Thus the fine interplay between  $E_{LR}$  and  $B$  plays a crucial role in the efficiency of the quantum search. While lattice vibrations are essential in locating the impurity site, these should not be too strong to disrupt the intermolecular cooperativity which determines the search process.

We emphasize two critical operations of the Grover's search which is satisfied by Eqs. (10) and (11). While Eq. (10) provides a local operation which distinguishes the impurity site from other sites, Eq. (11) provides an oracle-like operation which addresses only the impurity site via the evolution mechanism present in the Green's function formalism. The Green's function for an exciton at time  $t$  is given by [5, 16]

$$G(\mathbf{k}, t) = -i\langle 0 : n_{\mathbf{q}} | T \{ B_{\mathbf{k}}(t) U(t, 0) B_{\mathbf{k}}^\dagger(0) \} | 0 : n_{\mathbf{q}} \rangle \quad (13)$$

$$B_{\mathbf{k}}(t) = B_{\mathbf{k}}(0) \exp(iE(\mathbf{k}) t) \quad (14)$$

where  $|0 : n_{\mathbf{q}}\rangle$  denotes a state with  $n_{\mathbf{q}}$  phonons of wavevector  $\mathbf{q}$  and zero exciton population.  $T$  is the time ordering operator and  $U(t, 0)$  is the Dyson function

$$U(t, 0) = T \exp \left( -i \int_0^t \exp(i\hat{H}_T t') \hat{H}_{exp} \exp(-i\hat{H}_T t') dt' \right) \quad (15)$$

where  $\hat{H}_T$  and  $\hat{H}_{exp}$  are given in Eqs. (9) and (11). A direct relation between the Green's function  $G(k, t)$  in Eq. (13) and exciton energy  $E(\mathbf{k})$  has been derived by Craig et al [17] at  $t > 0$ ,

$$G(\mathbf{k}, t) = -i \exp[-i E(\mathbf{k}) t - \langle F \rangle] \quad (16)$$

At temperature close to  $T = 0\text{K}$ ,  $\langle F \rangle$  can be obtained in an explicit form [17, 18]

$$\langle F \rangle = \frac{1}{N} \sum_{\mathbf{q}} |\chi(q)|^2 \left[ -\frac{it}{\eta_{\mathbf{k}, \mathbf{q}}} + \frac{1}{\eta_{\mathbf{k}, \mathbf{q}}^2} (1 - \exp(i\eta_{\mathbf{k}, \mathbf{q}} t)) \right] \quad (17)$$

$$\eta_{\mathbf{k}, \mathbf{q}} = \hbar\omega(\mathbf{q}) + E_m - E(\mathbf{k}) - \Delta p \quad (18)$$

$E_m$  is the mean energy of the exciton band,  $N$  is the number of sites and the pre-factor  $\frac{1}{N}$  is due to the search for just one winner.

The imaginary component of the Green's function in Eq. (16) yields damping rate of the exciton transfer process among lattice sites. Here we use the damping rate to estimate the time needed to search for the impurity molecule,  $T_s$

$$\frac{1}{T_s} = \frac{1}{N} \sum_{\mathbf{q}} |\chi(q)|^2 \delta(\eta_{\mathbf{k}, \mathbf{q}}) \quad (19)$$

In order to obtain an explicit result for  $T_s$ , we assume that the phonon modes obey the Debye distribution with density of states given by  $\rho(\hbar\omega) = 3N(\hbar\omega)^2 / (\hbar\omega_D)^3$  where  $\omega_D$  is the Debye cutoff frequency. Using Eqs. (8), (12) and (19), we obtain an approximate expression for search time  $T_s$  at  $1 < \mu < \frac{3}{2}$

$$\frac{1}{T_s} = \frac{1}{T_0} + \frac{1}{T_N} \quad (20)$$

$$T_0 \approx \frac{\hbar E_0(\mu)}{3\pi E_{LR}} \left( \frac{\hbar\omega_D^2}{\Delta p^3} \right) \quad (21)$$

$$T_N \approx \frac{T_0}{A(\mu)'} N^{\mu-1} \quad (22)$$

where  $E_0(\mu)$  is the upper band-edge energy in Eq. (8). In order to highlight the explicit dependence of  $T_s$  on  $N$ , we have approximated energy of a single phonon,  $\hbar\omega(\mathbf{q}) \approx \Delta p$  instead of using the energy conservation relation in Eq. (18). The search time constitutes a  $N$ -independent term associated with the maximum bandwidth and dependent on the topological parameter  $\mu$  (see Eq. (8)), and a second Grover-like  $N$  dependent term which scales as  $N^{\mu-1}$ . Thus two concurrent mode of search mechanisms appears to be involved in Eq. (20), one associated with a quantum coherence effect that is independent of  $N$  and another term which has the well-known Grover-like search features [1]. At  $N \rightarrow \infty$ , we obtain a constant search time  $T_s = T_0$  for the system. We note that the maximum bandwidth associated with  $E_0(\mu)$  in Eq. (8) corresponds to a delocalized state of optimum coherence when the search is conducted from all lattice sites. At the peak of the energy band, the exciton can be considered to exist at all sites at the same time, in a maximally entangled state of existence. The search time  $T_0$  associated with the maximum bandwidth yields the fastest time and consequently the most efficient route to search the impurity site. For very large  $T_N \geq T_0$ ,  $T_s \sim T_0$ , the search route is dominated by the first coherent term in Eq. (20).

At the marginal  $\mu = \frac{3}{2}$ , we obtain a term that equivalent to the well-known Grover's search term,  $\propto N^{\frac{1}{2}}$  [1]. The Grover's algorithm result gives the maximal possible probability of finding the desired element [19]. However it only describes a specific mode to search a list of  $N$  sites and in this regard, the speedup features in the excess search term  $T_N$  of Eq. (20) at  $\mu < \frac{3}{2}$  is associated with the peculiarities of the level spacing (of order  $\Delta E \sim N^{-\mu+1}$ ) at the top band as discussed in Ref. [11]. This implies that the search proceeds with a decreasing number of target sites as the energy of the quasi-particle decreases. The explicit relation in Eq. (20) was obtained by utilizing a background boson field coupled with the evolution mechanism of the Dyson propagator (see Eq. (15)) within the Green's function formalism. Such an approach may facilitate search procedures with a number of channels for the delocalized excitation to pursue the preferred impurity site efficiently. The range of  $\mu$  considered here provide ideal conditions required to trap the exciton in the fastest time, when the quantum search is considered accomplished. In contrast to the dynamics at the top of the exciton band, it was shown that the energy level spacing scales as  $\Delta E \sim N^2$  at the bottom band [11]. This means that the search for a target site located at a higher level would experience a slowdown effect as is obvious when substituting higher  $\mu$  values in Eq. (20). The parallels between the quantum search mechanism and physical processes considered so far is shown in Table 1.

**Table 1** *Parallels between exciton trapping mechanism and the proposed Grover-like search problem*

Physical State/Process	Implementation
Ideal crystal in Vacuum state	Null state $ 0\rangle^{\otimes N}$
Photon Absorption	Hadamard-like transformation
Delocalized exciton	Entangled state
Isotopic impurity molecule	Grover's Target state ("Winner")
Total number of molecules	System size
Phonon field	Marks Target state
Exciton-phonon interaction operator	Oracle-like action
Dyson propagator	Assists Quantum Search
Expt. measurement(e.g. Fluorescence)	Search Ends
Annihilation or relaxation processes	Sources of Error
Quantum Zeno Effect	Error Minimization

### Organic molecular systems with $\mu = 3$ .

It is important to note that the marginal exponent  $\mu = \frac{3}{2}$  is not expected in any known molecular system, nevertheless in organic systems such as Frenkel excitons in Langmuir-Blodgett films, molecules experience dipole-type exchange mechanisms with  $\mu = 3$  [5, 7]. For such systems, the exciton bandwidth expression in Eq. (8) is modified as [12]

$$B(K) \approx E_0(\mu)(1 - A(\mu)'N^{-2}) \quad (23)$$

for ( $\mu > 3$ ). Using Eqs. (23), (12) and (19), we obtain

$$\frac{1}{T_s} \approx \frac{1}{T_0} + \frac{1}{T_N} \quad (24)$$

$$T_N \approx \frac{T_0}{A(\mu)'}N^2 \quad (25)$$

where  $T_0$  is given in Eq. (20). We use crystal parameters for the naphthalene host crystals ( $C_{10}H_8$ ) doped with isotopic impurities used in an earlier work [20], with  $\Delta p \approx 50\text{cm}^{-1}$ ,  $\hbar\omega_D \sim E_0(\mu) \approx 90\text{cm}^{-1}$  and  $E_{LR} = 0.004$  eV. For  $N = 10^2$  and  $\mu = 3$ , we obtain search times  $T_0 \approx 0.01\text{ps}$ ,  $T_N \approx 10 - 100\text{ps}$  and overall  $T_s \approx 0.01\text{ps}$ . The vast difference in search times,  $T_0$  and  $T_N$  suggests that the search route in organic systems may be dominated by the first coherent term in Eq. (24). Delayed fluorescence techniques [21] may be used to detect the impurity site and confirm the results obtained here. The emission of fluorescence during experimental measurement can be considered to signal the end of the quantum search. Recent advances in spectroscopic techniques [22] may be used to verify the femtosecond time scale estimates predicted for  $T_0$  in naphthalene doped organic systems. Studies of exceptionally efficient excitation transfer in photosynthetic systems has also been explored in recent works [9]. In this regard, there is possible application of the coherent size-independent, connectivity dependent time component  $T_0$  derived in Eq. (20) to studies related to excitation transfer in photosynthetic systems and associated phenomenon of quantum photosynthesis.

### PROCESSES WHICH COMPETE WITH GROVER-LIKE SEARCH PROCESS

In this section, we consider various sources of decoherence-type mechanisms that will result in improper search patterns of the impurity site.

## Downward relaxation and decoherence of superposed exciton states

Exciton-phonon scattering can interfere with the search process by causing downward relaxation of states which occupy the upper exciton band levels. The possibility of such a process can be minimized by ensuring that the exciton remains delocalized and hence entangled over a number of molecular sites with size equivalence to the overall number of sites to be searched. In the presence of decoherence effects due to lattice vibrations, it is thus imperative that the coherent length associated with the superposed exciton state in Eq. (1) should at least exceed the number of sites to be searched. This means that the exciton state should retain its coherent form at least for the time needed for the exciton to reach the target impurity site, a condition best described by the relation

$$T_N < T_{\text{scat}} \quad (26)$$

where  $T_{\text{scat}}$  is the scattering time. Using perturbation theories, the scattering rate can be estimated using  $T_{\text{scat}} \sim E_{LR}k_B T \rho(E)$  where  $\rho(E)$  is the normalized density of states of the unperturbed lattice system[8]. For a constant density within the band  $(\Delta E - B, \Delta E + B)$ ,  $\rho(E) = \frac{1}{\sqrt{B^2 - E^2}} \sim \frac{1}{2B}$  at  $\mu = 3$ . The density of states,  $\rho(E)$  is highly sensitive to the parameter  $\mu$  which appears in Eq. (6) [12]. For  $\mu = 3$ , we obtain

$$T_{\text{scat}} \approx \frac{\hbar B}{E_{LR}k_B T} \quad (27)$$

where  $E_{LR}$  the lattice relaxation energy is defined in Eq. (12) and  $B$  denotes the half band width. Comparing Eq. (27) with Eqs. (21) and (22), and substituting the upper band-edge energy  $E_0(\mu) = 2B$  and  $A(\mu)' \approx 1$ , we obtain an explicit condition required for the Grover-like search to proceed successfully without being affected greatly by downward relaxation

$$N^2 < \frac{3\pi\Delta p^3}{k_B T \hbar \omega_D^2} \quad (28)$$

The number of sites that can be searched without disruption increases at low temperatures and at higher trap depth,  $\Delta p$ . We bear in mind, however the possibility that the impurity energy band may become disengaged from the exciton band with significant loss in translational symmetry due to deep traps associated with very large  $\Delta p$ .

Another undesirable effect associated with exciton-phonon scattering is the introduction of composite exciton-phonon characteristics to the exciton bandstructure. It can be seen that a fixed sum of exciton and phonon wavevectors given by  $\mathbf{K} = \sum_{\mathbf{k}, \mathbf{q}} (\mathbf{k} + \mathbf{q})$ , involves an infinite number of phonons with wavevector  $\mathbf{q}$ . This leads to a weakening effect of an impurity trap due to interference. For instance, the presence of an isotopic impurity displaces the energy band by  $E = \sqrt{B^2 + \Delta p^2}$ , so that at bandwidth  $B = 300\text{cm}^{-1}$  and  $\Delta p \approx 100\text{cm}^{-1}$  we obtain an energy shift of about  $\Delta E = 16\text{cm}^{-1}$  below the band-edge. At temperatures higher than 30K, it is not uncommon for appearance of band spectra features of the order  $\sim 10\text{cm}^{-1}$  [5], this implies that exciton-phonon coupling leads to comparable energy shifts as the impurity state. Therefore exciton-phonon relaxation may produce “defective” winners. Hence operating at the right temperatures holds the key to maintaining a fine balance between undesirable features of phonons and its facilitating role in energy transport. The calculations above that at temperatures close to 5K, we expect a clear distinction between “defective” and “genuine” winners when the exciton are trapped at the impurity states displaced from the exciton band. Another side effect of  $T_{\text{scat}}$  is manifested in the the phase coherence in Eq. (2) which becomes increasingly damped at higher temperatures

$$B_{\mathbf{K}}^\dagger = N^{-1/2} \sum_{\mathbf{l}} e^{i(\mathbf{K} + i\mathbf{k}') \cdot \mathbf{l}} B_{\mathbf{l}}^\dagger = N^{-1/2} \sum_{\mathbf{l}} e^{i\mathbf{K} \cdot \mathbf{l}} e^{-\mathbf{k}' \cdot \mathbf{l}} B_{\mathbf{l}}^\dagger \quad (29)$$

It is well known that the imaginary component  $k'$ , which appears as a result of the scattering mechanism in Eq. (27), is a source of decoherence in the entangled exciton state.

For the naphthalene host crystals ( $\text{C}_{10}\text{H}_8$ ), typical value of  $B \sim 100\text{cm}^{-1}$ , and using  $k_B T = 3.7\text{meV}$  at  $T = 30\text{K}$ , we obtain  $T_{\text{scat}} \approx 50\text{ps}$  which reduces to 500ps at a lower  $T = 5\text{K}$ . These times are comparable to the search time  $T_N \approx 100\text{ps}$  obtained earlier, suggesting that downward relaxation mechanism may pose as a serious drawback to the Grover’s search mechanism at increasing temperatures ( $T > 10\text{K}$ ). It should noted that  $T_0$  (see Eq. (21)) associated with the maximum bandwidth and with coherence properties still remains the dominant pathway to energy transfer due to the very fast times  $T_0 \approx 0.01\text{ps}$  computed earlier for naphthalene crystal system in comparison to the Grover’s search term  $T_N$  (see Eq. (22)) as well as  $T_{\text{scat}}$ .

### Exciton formation at impurity site

It is possible that an exciton is created at an impurity site due to the binding of free charge carriers instead of trapping of an exciton participating in the Grover-like search mechanism. In this section, we compute the rates associated with such a process which acts to disrupt the search process. In Frenkel excitons, both charge carriers are generally created via optical excitation on the same molecule. The transition from the initial state of charge carriers to a final state of trapped exciton via acoustic phonon occurs as

$$\mathbf{e} + \mathbf{h} \longrightarrow \overset{\circ}{\mathbf{h}} + \hbar\omega, \quad (30)$$

where  $\mathbf{e}$ ,  $\mathbf{h}$  and  $\overset{\circ}{\mathbf{h}}$  denote a free electron, hole and exciton respectively, and  $\hbar\omega$  is the frequency of an acoustic phonon. The initial and final states appear as

$$\begin{aligned} |i\rangle &= \sum_{\sigma_e, \sigma_h} a_{\mathbf{k}}^\dagger(\sigma_e) d_{\mathbf{K}-\mathbf{k}}^\dagger(\sigma_h) |0; n\rangle \\ |f\rangle &= B_{\mathbf{K}-\mathbf{q}}^\dagger(\sigma_S) b_{\mathbf{q}}^\dagger |0; n\rangle \end{aligned} \quad (31)$$

where  $\sigma_e(\sigma_h)$  denotes the electron (hole) spin, while the lowest internal exciton state is assumed with spin  $\sigma_S = 0(1)$  for the singlet (triplet) state [23].  $a_{\mathbf{k}}^\dagger(d_{\mathbf{k}}^\dagger)$  denote the electron (hole) creation operator of wavevector  $\mathbf{k}$  in their respective energy bands. The exciton wavevector can be written as a linear combination of all eigenvectors of the free charge carriers (see Eq. 3 in Ref.[23]). The initial and final state eigenvalues are obtained using

$$\begin{aligned} E_i &= W_0 + E_g + \frac{\hbar^2 \mathbf{k}^2}{2m_e^*} + \frac{\hbar^2 (\mathbf{K} - \mathbf{k})^2}{2m_h^*} + \Gamma_{ph} \\ E_f &= W_0 + E_g + \Delta p + \frac{\hbar^2 (\mathbf{K} - \mathbf{q})^2}{2M^*} + \hbar\omega(\mathbf{q}) + \Gamma_{ph} \end{aligned} \quad (32)$$

where  $\Gamma_{ph}$  represents the phonon energy that remains unchanged during the transition and  $W_0$  is the total electronic energy of crystal with all molecule in their ground states.  $m_e^*, m_h^*$  and  $M^*$  are the respective effective masses of the electron, hole and exciton. The rate of formation of the exciton at the impurity site is evaluated using the following exciton-impurity-phonon interaction operator

$$\hat{H}_{imp} = \Delta p N^{-1} \sum_{\mathbf{k}, \mathbf{k}', \mathbf{q}} \left[ \frac{\hbar}{2I_p \omega(\mathbf{q})} \right]^{1/2} (\mathbf{k} - \mathbf{k}') \cdot \hat{e}(\mathbf{q}) \exp[i(\mathbf{k}' - \mathbf{k} + \mathbf{q}) \cdot \mathbf{p}] B_{\mathbf{k}}^\dagger B_{\mathbf{k}} (b_{\mathbf{q}}^\dagger + b_{\mathbf{q}}), \quad (33)$$

where  $\hat{e}$  is the unit polarization wavevector and  $I_p$  is the mass coefficient of the impurity molecule which we assume to the same as the mass coefficient of the host molecules. The rate of formation of an exciton at the impurity site is calculated using

$$R_f = \frac{n_i}{\hbar} \sum_{\mathbf{k}, \mathbf{q}} |\langle f | \hat{H}_{imp} | i \rangle|^2 \delta(E_f - E_i) \quad (34)$$

where  $n_i$  denotes the concentration of free charge carriers. For the singlet exciton ( $\sigma_S = 0$ ), we obtain using Eq. (31),(32) and (34) an explicit expression for the exciton formation rate at low temperatures

$$\frac{1}{T_f} = R_f \approx \frac{2n_i m_e^* N^* d_0}{\hbar^2 \xi v} [(E_T - E_b)^2 + \Delta p^2] \quad (35)$$

where  $N^*$  and  $d_0$  are the number of molecular sites and inter-molecular distance respectively at an edge of the crystal unit cell.  $E_T$  is the transport gap, the minimum energy required for the formation of a free electron and hole pair,  $E_b$  is the binding energy,  $\xi$  is mass density of the host molecules and  $v$  denotes the velocity of sound in the crystal.

For naphthalene host crystals ( $C_{10}H_8$ ) doped with isotopic impurities, we use  $\Delta p \approx 50 \text{cm}^{-1}$ ,  $(E_T - E_b) = 3 \times 10^4 \text{cm}^{-1}$ ,  $n_i \sim 10^{15} \text{cm}^{-3}$ ,  $\xi = 1283 \text{kg m}^{-3}$ ,  $v = 10^4 \text{cm s}^{-1}$ ,  $N \times d_0 = 7.8 \times 10^{-10} \text{m}$ , and obtain  $T_f \approx 10^{-9} \text{s}$ . We note the crucial dependence of the formation rate on the carrier concentration, however even with a large carrier concentration  $n_i$ , a comparatively slow error time is obtained. This can be attributed to the large bandgap in molecular systems, with the requirement that charge carriers have to be optically generated the probability of exciton formation at the impurity site is less likely at low excitation intensities. Moreover due to the large binding energies of the Frenkel exciton, participation of phonons of relatively higher energies is needed before excitons can be formed at the impurity site, dissimilar to the situation in semiconductors [24]. We can therefore conclude that exciton formation at impurity site is not disruptive to the proposed Grover's like search mechanism, at least in naphthalene -doped organic crystals.



### Exciton-exciton annihilation.

Excitons in close proximity can dissociate due to electrostatic interactions, creating free charge carriers. The energy released from recombination of an electron and a hole bounded together as an exciton at one molecular site can lead to dissociation of exciton at another site, with possible participation of phonons. Such a process can compete with the proposed Grover-like search process, hence we examine exciton-exciton annihilation between two free excitons *prior* to exciton trapping at the impurity site. For simplicity, we consider the two interacting excitons to be in the singlet spin state ( $\sigma_S = 0$ ), the generated hole carrier to be trapped at a site leaving only the electron free after annihilation. The conservation of momentum rule ensures that the exciton momentum is transferred to electron after the annihilation process, in which participation of phonons are omitted. Due to the small phonon participation number, the order of magnitude of the annihilation rates are not greatly affected by omission of interaction terms associated with phonons. We write the eigenvectors of the initial and final states as

$$|i\rangle = B_{\mathbf{K}_1}^\dagger B_{\mathbf{K}_2}^\dagger |0; n\rangle \quad (36)$$

$$|f\rangle = \sum_{\sigma_e, \sigma_h} a_{\mathbf{k}}^\dagger(\sigma_e) d_{\mathbf{k}'}^\dagger(\sigma_h) |0; n\rangle \quad (37)$$

where  $a_{\mathbf{k}}^\dagger$  ( $d_{\mathbf{k}}^\dagger$ ) which denote the electron (hole) creation operators are associated with free charge carriers. The transition from  $|i\rangle$  to  $|f\rangle$  is enabled by electrostatic interactions  $V_{mn}$  between molecules  $m$  and  $n$  with a transition matrix of the form

$$\begin{aligned} \langle f | \hat{V} | i \rangle &= 2N^{-1} \sum_{\mathbf{l}, \mathbf{n}} \exp[\mathbf{k} \cdot (\mathbf{n} - \mathbf{l})] \\ &\times \left[ \langle \mathbf{0}, \mathbf{m}; \mathbf{e} + \mathbf{h}, \mathbf{l} | V_{mn} | \begin{smallmatrix} \mathbf{e} \\ \mathbf{h} \end{smallmatrix}, \mathbf{n}; \begin{smallmatrix} \mathbf{e} \\ \mathbf{h} \end{smallmatrix}, \mathbf{m} \rangle - \frac{1}{2} \langle \mathbf{e} + \mathbf{h}, \mathbf{l}; \mathbf{0}, \mathbf{n} | V_{mn} | \begin{smallmatrix} \mathbf{e} \\ \mathbf{h} \end{smallmatrix}, \mathbf{n}; \begin{smallmatrix} \mathbf{e} \\ \mathbf{h} \end{smallmatrix}, \mathbf{m} \rangle \right] \end{aligned} \quad (38)$$

The first term within the square bracket describes recombination of a free exciton (denoted by  $\begin{smallmatrix} \mathbf{e} \\ \mathbf{h} \end{smallmatrix}$ ) at site  $\mathbf{m}$ , with the released energy inducing the exciton at  $\mathbf{n}$  into a pair of free carriers (denoted by  $\mathbf{e} + \mathbf{h}$ ) at site  $\mathbf{l}$ . A similar interpretation holds for the second term, with recombination of the free exciton taking place at site  $\mathbf{n}$  instead. The initial and final state energies are obtained as

$$E_i = W_0 + 2E_0(K) + \frac{\hbar^2 K^2}{2M^*} \quad (39)$$

$$E_f = W_0 + E_e(K) + \frac{\hbar^2 K^2}{2m_e^*} \quad (40)$$

$W_0$  is the total electronic energy of crystal with all molecule in their ground states and  $E_0(K)$  is the exciton energy given in Eq. (5).  $E_e(K)$  denotes the free electron energy. Using the Golden Rule formula of Eq. (34) as well as Eqs. (38) and (39), we obtain the exciton-exciton annihilation rate  $R_{an}$  as

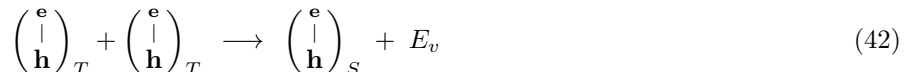
$$\frac{1}{T_{an}} = R_{an} \approx \frac{10 n_{ex}}{\hbar^4} \left[ m_e^{*3/2} E_T^{5/2} N^{*6} d_0^6 \right] \quad (41)$$

where  $n_{ex}$  is the concentration of free excitons and  $N^*$  and  $d_0$  are defined below Eq. (35).  $E_T$ , the transport gap is used to estimate the square of the transition matrix in Eq. (38). This approximation is justified as Eq. (38) describes transition associated with the energy required for the formation of a free electron and hole pair as quantified by the transport gap.

We estimate the exciton-exciton annihilation rate  $R_{an}$  for the naphthalene host crystals ( $C_{10}H_8$ ) using  $E_T = 3 \times 10^4 \text{cm}^{-1}$ ,  $n_{ex} \sim 10^{12} \text{cm}^{-3}$ ,  $\xi = 1283 \text{kg m}^{-3}$ ,  $N \times d_0 = 7.8 \times 10^{-10} \text{m}$ , and obtain  $T_{an} = \frac{1}{R_{an}} \approx 10^{-11} \text{s}$ . Thus exciton-exciton annihilation time  $T_{an}$  is comparable to the Grover-like search time,  $T_N \approx 100 \text{ps}$  at high concentration of free excitons. At even higher exciton concentration  $n_{ex} > 10^{15} \text{cm}^{-3}$ , this process may dominate the exciton dynamics leading to a breakdown of the Grover-like search process. Hence it is imperative that the exciton concentration is set low so that exciton-exciton annihilation is not disruptive to the search process, in naphthalene-doped organic crystals. We note the crucial dependence of  $R_{an}$  on  $N^*$ , which yields a measure of packing density of the searched sites. Hence the distribution of searched sites plays an important role in the influence of exciton-exciton annihilation, which is expected intuitively as well.

### Exciton fusion and fission.

During exciton fusion, two triplet excitons combine to form a singlet exciton as shown below



The subscripts  $T$  and  $S$  correspond to the triplet and singlet exciton respectively, with excess energy  $E_v$  generally released as molecular vibrations. In naphthalene organic system, the energy difference between two triplet excitons and a singlet exciton is given by  $2E(\sigma_S = 1) - E(\sigma_S = 0) = E_v = 1.3$  eV, with the triplet exciton energy tending to decrease faster than the singlet exciton [25]. A reverse process in which a singlet exciton undergoes conversion into a pair of triplet excitons is termed exciton fission. Hence in the fusion (fission) process, a singlet (triplet) exciton is formed with all excess energy is released (absorbed) via intra- or inter- molecular vibrations. The calculation of rates of exciton fission or fusion is similar to that for exciton-exciton annihilation for which free charge carriers were created in the final state (see Eq. (40)). We therefore do not give quantitative details of the process, however we note the sensitive dependence of such processes on  $n_{ex}$ , the concentration of free excitons as obtained in Eq. (41). This was also noted in a recent work with rates estimated in the picosecond range  $\sim 1 - 10$  ps for closely related naphthalene-related systems [26]. We expect that at low exciton concentration and packing density of the searched sites  $N^*$ , exciton fusion and fission processes are less likely to disrupt the overall dynamics involved in the Grover's like search process.

### EXCITON DYNAMICS CONTROL VIA THE ZENO EFFECT.

Quantitative estimates for the naphthalene doped organic systems show that several mechanisms, in particular downward relaxation due to exciton-phonon interaction, exciton-exciton annihilation, exciton fusion and fission process become dominant at raised temperatures and high exciton concentration which translates as packing density of the searched sites. Overall we note that the coherent term  $T_0$  in Eq. (21) associated with the maximum bandwidth still remains the dominant pathway to energy transfer in comparison to the Grover's search term  $T_N$  (Eq. (22)), relaxation term  $T_{\text{scat}}$  (Eq. (27)), formation time  $T_f$  (Eq. (35)) and exciton-exciton annihilation time,  $T_{\text{an}}$  (Eq. (41)). Nevertheless, the exciton dynamics associated with Grover's search term  $T_N$  can be carefully harnessed via the quantum Zeno effect [27]. This effect embodies the controlling effect of a measurement process whereby a system monitored to determine whether it remains in a particular state resists making transitions to alternate states. In recent years, this idea has been studied using an adiabatic theorem [28, 29] in which different outcomes are eliminated and the system evolves as a group of exclusive quantum Zeno subspaces within the total Hilbert space. The quantum Zeno effect can be utilized to exclusively direct the Grover-like search process to proceed uninterrupted while suppressing alternate mechanisms of exciton transport and dynamics. Such directed control of many-body dynamics via Zeno effect has been experimentally demonstrated in recent works [30, 31], with potential applications in quantum information systems. We are unaware of the use of Zeno effect to switch selected interactions "on and off" in molecular systems.

### SEARCH ON A FLUCTUATING LONG-RANGE INTERACTING CYCLE (LRIC) GRAPH LATTICE

A long-range interacting cycle (LRIC) graph is an extension of the nearest-neighbor model and a simpler variant of the model considered earlier in Eq. (6). In a LRIC graph lattice, all two nodes of distance  $m$  are connected [32], a key feature which ensures that all lattice sites have the same connectivity of 4. These newly added edges serve as shortcuts in the cycle graph, and serve to increase the cross paths and hence bandwidth  $B$  of the lattice system. The one-dimensional LRIC graph lattice is denoted by two parameters,  $N$  and  $m$  and the exciton Hamiltonian present in such a lattice appear as

$$\hat{H}_{ex} = \sum_l E_l B_l^\dagger B_l + J \sum_l B_l^\dagger B_{l+1} + J \sum_l B_l^\dagger B_{l-1} + J \sum_l B_l^\dagger B_{l+m} + J \sum_l B_l^\dagger B_{l-m} \quad (43)$$

where  $E_l$  denotes the onsite energy and  $J > 0$ , and the intersite energy is assumed to be independent of the distance between any two sites. Using the Fourier transform in Eq. (2), the eigenenergies are obtained as  $E_{n,m} = \Delta E + 2J(\cos K + \cos mK)$  with momenta  $K = \frac{2\pi k}{N}$  within the Brillouin zone  $k \in [1, N]$ . The LRIC Hamiltonian is diagonal

in  $K$  space

$$\hat{H}_{ex} = \sum_K E_{n,m}(K) B_K^\dagger B_K \quad (44)$$

The bandwidth  $B$  of a Frenkel exciton in a LRIC lattice therefore has a simple form  $B = 2J \cos K + 2 \cos mK$ . We now consider that the lattice points of a LRIC graph undergo small vibrations, and using the Green's function approach considered in the earlier Section, we can examine the effect of  $m$  on the search time. We consider a large  $N$  so that the impurity trap falls within the bandwidth  $B$ . The exciton bandwidth is also considered to include the acoustic phonon bandwidth. At small  $m$ ,  $B(K \rightarrow 0, N \rightarrow \infty) \approx 2J(1 - (\frac{2\pi m}{N})^2)$  and using Eq.(19), we obtain a search time component  $T_N$  that scales as  $N^2$ . However for large  $m$ , the bandwidth oscillates strongly depending on  $m$ . Using  $N = pm$  where integer  $p$  provides a measure of the lattice network extension, and considering small values of  $\cos mK$ , we obtain

$$\begin{aligned} \frac{1}{T_s} &\approx \frac{1}{T_0} - \frac{1}{T_N} \\ T_p &\approx \frac{T_0}{\cos(\frac{2\pi}{p})} \end{aligned} \quad (45)$$

where as in Eq.(20),  $T_0$  is an  $N$ -independent term. The search time component  $T_p$  decreases gradually with  $p$  so that search time  $T_s$  increases overall as is expected with an increasing lattice network extension. We note that  $T_s$  in Eq. (45) does not resemble the Grover-like form obtain earlier in Eq. (19), due to the vast reduction in exciton delocalization property associated with the simpler exciton Hamiltonian structure of the LRIC graph lattice. Nevertheless the explicit dependence of search time  $T_s$  on  $p$  illustrates the importance of the efficiency of excitation transfer in quantum searches. The search time  $T_s$  is optimum for large  $m$ , which agrees well with the result that the exciton survival probability decays faster on networks of large  $m$  [32].

## DISCUSSION AND CONCLUSION

We have demonstrated the plausibility of a Grover-like search problem by means of Frenkel exciton trapping process at a shallow isotopic impurity. We have considered several mechanisms which may compete on equal terms with our proposed Grover's search mechanism. Quantitative estimates for the naphthalene doped organic systems show that Grover's search mechanism remains plausible under suitable conditions and may be physically implemented with assistance from Zeno effect. We emphasize the striking resemblance of a derived explicit term for exciton trapping time to the well-known Grover's search time, which includes notable speedup features in the characteristic range  $1 < \mu < \frac{3}{2}$  for a graph lattice with long-range intersite interactions. These parameters provide optimum conditions required to trap the exciton in the fastest time. We suggest use of Zeno effect associated with experimental measurements as a viable means of eliminating ubiquitous disruptive interactions and harnessing the search process, with emission of fluorescence signifying the end of a quantum search.

A recent work on light-harvesting networks [33] showed the role of network size and connectivity as critical factors which lead to optimum energy transfer in graph lattice systems, and our results agree well with this observation. We emphasize the significance of a derived connectivity dependent time component  $T_0$ , associated with intermolecular cooperativity and coherence properties of the entangled exciton as a dominant source of excitation transfer mechanism. The derived explicit term can be utilized to examine high efficiencies of energy transfer in photosynthetic systems [9]. Estimates of various search times and excitonic mechanisms obtained in this work can be verified by experiments employing fast femtosecond time resolution spectroscopic techniques [22]. Finally, our results show that the natural evolution mechanism of the Dyson propagator within the Green's function formalism may play a critical role in the construction of efficient quantum search devices, and in bridging the gap between excitonic theory and its use in quantum information processing.

## ACKNOWLEDGMENTS

I gratefully acknowledge useful comments from the anonymous referee.

---

\* Electronic address: thilaphys@gmail.com

- [1] L. K. Grover, Phys. Rev. Lett. **79**, 325 (1997).
- [2] S. Aaronson and A. Ambainis, quant-ph/0303041, Proc. 44th IEEE Symposium on Foundations of Computer Science, 200 (2003).
- [3] E. Farhi and S. Gutmann, Phys. Rev. A **58**, 915 (1998).
- [4] A. Childs, E. Farhi, S. Gutmann, Quantum Information Processing **1** 35 (2002).
- [5] A. S. Davydov, *Theory of Molecular Excitons* (Plenum, New York, 1971).
- [6] F. C. Spano, Phys. Rev. B **46**, 13017 (1992).
- [7] D. P. Craig and S. H. Walmsley, *Excitons in Molecular Crystals* (Benjamin Inc., New York, 1968).
- [8] Y. Toyozawa, *Optical Processes in Solids* (Cambridge, New York, 2003).
- [9] A. Olaya-Castro, Chiu Fan Lee, F. F. Olsen and N. F. Johnson, Phys. Rev. B **78**, 085115(2008).
- [10] M. Dalai, Recurrence relations for the Lerch  $\Phi$  function and applications, Journal for Analysis and its Applications **24**, 895 (2005).
- [11] A. Rodríguez, V. A. Malyshev, G. Sierra, M. A. Martin-Delgado, J. Rodríguez-Laguna and F. Domínguez-Adame, Phys. Rev. Lett. **90**, 027404 (2003).
- [12] D. B. Balagurov, V. A. Malyshev and F. Domínguez-Adame, Phys. Rev. B **69**, 104204 (2004).
- [13] F. A. B. F. de Moura, A. V Malyshev, M. L. Lyra, V. A. Malyshev, and F. Domínguez-Adame, Phys. Rev. B **71**, 174203 (2005).
- [14] A. M. Childs and J. Goldstone, Phys. Rev. A **70**, 022314 (2004).
- [15] D. Deutsch and R. Jozsa, *Rapid solution of problems by quantum computation* Proc. Roy. Soc. Lond. A, **439**, 553 (1992).
- [16] A. Suna, Phys. Rev. **135**, A111 (1964).
- [17] D. P. Craig and M. R. Philpott, Proc. Roy. Soc. A **290**, 583 (1966).
- [18] D. P. Craig, L. A. Dissado and S. H. Walmsley, Chem. Phys. Lett. **46**, 191 (1977).
- [19] C. Zalka, Phys. Rev. A **60**, 2746 (1999).
- [20] J. Singh and A. Thilagam, J. Lumin. **38**, 317 (1987).
- [21] J. L. Fave, C. Guthmann, M. Schott and H. Bouchriha, Phys. Rev. B **24**, 4545 (1981).
- [22] F. Milota, J. Sperling, A. Nemeth and H.F. Kauffmann, Chem. Phys. **357**, 45 (2009).
- [23] A Thilagam and M A Lohe J. Phys.: Condens. Matter **18**, 3157 (2006).
- [24] I.-K. Oh, Jai Singh, A. Thilagam and A. S. Vengurlekar, Phys. Rev. B **62**, 2045 (2000).
- [25] C. Jundt, G. Klein, B. Sipp, J. Le Moigne, M. Joucla, and A. A. Villaeys, Chem. Phys. Lett. **241**, 84 (1995).
- [26] A. Benfredj, F. Henia, L. Hachani, S. Romdhane, and H. Bouchriha, Phys. Rev. B **71**, 075205, (2005).
- [27] B. Misra and E. C. G. Sudarshan, J. Math. Phys. **18**, 756 (1977).
- [28] P. Facchi and S. Pascazio, Phys. Rev. Lett. **89** 080401 (2002).
- [29] A. Thilagam, *Zeno-anti-Zeno crossover dynamics in a spin-boson system*, (2010, under review).
- [30] M. Yamaguchi, T. Asano and S. Noda, Optics Express, **16**, 18067 (2008).
- [31] A. Laucht, F. Hofbauer, N. Hauke, J. Angele, S. Stobbe, M. Kaniber, G. Böhm, P. Lodahl,, M. C. Amann and J. J. Finley, New J. Phys. **11**, 023034 (2009).
- [32] Xin-Ping Xu, Phys. Rev. E **79**, 011117 (2009).
- [33] K. M. Gaab and C. J. Bardeen, J. Chem. Phys. **121**, 7813 (2004).